Optical Spectroscopy and Upconversion Studies of Ho 3+ −Doped Bulk and Nanocrystalline Y 2 O 3

ARTICLE *in* CHEMISTRY OF MATERIALS · JULY 2002

Impact Factor: 8.35 · DOI: 10.1021/cm011584m

Optical Spectroscopy and Upconversion Studies of Ho^{3+}-Doped Bulk and Nanocrystalline Y_2O_3

J. A. Capobianco,*,† J. C. Boyer,† F. Vetrone,† A. Speghini,‡ and M. Bettinelli‡

Department of Chemistry and Biochemistry, Concordia University, 1455 de Maisonneuve Boulevard W, Montreal, Quebec H3G 1M8, Canada, and Dipartimento Scientifico e Tecnologico, Università di Verona, and INSTM, UdR Verona, Ca' Vignal, Strada Le Grazie 15, 37134 Verona, Italy

Received October 30, 2001. Revised Manuscript Received February 20, 2002

In this paper we report on the optical spectroscopy and upconversion studies of Ho^{3+}-doped nanocrystalline and bulk Y_2O_3, as a function of holmium concentration (0.1, 0.5, 1, 2, 5, and 10 mol %). Emission in the blue, green, red, and NIR portions of the spectrum is recorded after 457.9-nm excitation. Red (646 nm) pumping results in blue and green emission through a two-photon excited-state absorption (ESA) upconversion process. NIR (754 nm) pumping results in blue, green, and red emission. Overall luminescence of the nanocrystalline samples under one-photon excitation or 646-nm pumping is severely reduced when compared to that of the bulk sample, or nonexistent in the case of the 754-nm pumping, which is attributed to adsorbed atmospheric carbon dioxide and/or water on the surface of the nanocrystals. A quenching of the green ($^5F_4$, $^5S_2$) → $^5I_8$ emission is noted with increasing Ho^{3+} concentration that is attributed to a cross-relaxation mechanism involving two holmium ions.

1. Introduction

Recent advances in flat-panel display technology have ignited the search for new powdered phosphors with nanometer dimensions. Currently, phosphors in the micrometer-size range find applications in a wide variety of information display devices such as cathode-ray tubes (CRTs), field emission displays (FEDs), vacuum fluorescent displays (VFDs), and electroluminescent (EL) devices.[1] It is anticipated that the advent of nanosized phosphors will lead not only to improved resolution but also to an increase in luminescent efficiency. A class of materials that has shown considerable promise in delivering these qualities are doped nanocrystalline materials.

Since the early 1990s, research in the field of nanocrystalline materials has grown markedly with more articles being published on the topic every year. Nanocrystalline materials are usually defined as polycrystalline solids with particle diameters or grain sizes ranging from sub-nanometers up to 100 nm. This innovative class of materials demonstrates striking particle-size-dependent phenomena that affect the following: (i) emission lifetime; (ii) luminescence quantum efficiency; and (iii) concentration quenching. As the size of the crystal decreases, there is a continuous transition from bulk to molecular properties with a number of these effects being attributed to quantum confinement or more generally to restricted geometry.

A subgroup of nanocrystalline materials that has attracted considerable attention for use as potential phosphors are rare-earth-doped yttrium oxide (Y_2O_3) nanocrystals. Micrometer-sized Y_2O_3:Eu^{3+} phosphors have been used since the 1970s as the red component in television projection tubes and fluorescent lighting devices.[2] Recently, numerous studies have focused on the optical properties of nano-dimensioned Y_2O_3:Eu^{3+}.[3−7] Tissue and co-workers have thoroughly investigated and reported results on Eu^{3+}-doped monoclinic Y_2O_3, noting changes in the luminescent spectra and lifetime of the red $^5D_0$ → $^7F_2$ transition with decreasing particle size.[7]

Upconversion is a process by which excitation to lower lying levels with low-energy radiation (e.g., near-infrared radiation) results in higher energy emission (e.g., visible and near UV radiation) from higher electronic levels.[8] This process requires the absorption of at least two photons to provide sufficient energy for the upconverted emission to occur. When certain rare-earth-ion impurities such as Er^{3+}, Ho^{3+}, and Tm^{3+} are introduced in sufficient concentrations into a suitable host lattice, they are capable of upconverting infrared radiation to various shorter wavelengths. The recent advent of low-cost near-infrared (NIR) laser diodes has generated interest in upconversion materials for uses

* To whom correspondence should be addressed. Telephone: 514-848-3350. Fax: 514-848-2868. E-mail: capo@vax2.concordia.ca.
† Concordia University.
‡ Università di Verona.

(1) Shea, L. E.; McKittrick, J.; Lopez, O. A. *J. Am. Ceram. Soc.* **1996**, *79*, 3257−3265.
(2) Franz, K. A.; Kehr, W. G.; Siggel, A.; Wieczoreck, J. In *Ullman's Encyclopedia of Industrial Chemistry*; Elvers, B., Hawkins, S., Schulz, G., Eds.; VCH Publishers: Weinheim, Germany, 1985; Vol. A15.
(3) Eilers, H.; Tissue, B. M. *Chem. Phys. Lett.* **1996**, *251*, 74−78.
(4) Ye, T.; Guiwen, Z.; Weiping, Z.; Shangda, X. *Mater. Res. Bull.* **1997**, *32*, 501−506.
(5) Tissue, B. M. *Chem. Mater.* **1998**, *10*, 2837−2845.
(6) Williams, D. K.; Bihari, B.; Tissue, B. M.; McHale, J. M. *J. Phys. Chem. B* **1998**, *102*, 916−920.
(7) Williams, D. K.; Yuan, H.; Tissue, B. M. *J. Lumin.* **1999**, *83−84*, 297−300.
(8) Auzel, F. E. *Proc. IEEE* **1973**, *6*, 758.

10.1021/cm011584m CCC: $22.00
Published on Web 06/04/2002

in all-solid-state visible lasers. These materials have other possible applications such as phosphors emitting in the visible spectral range, in solid-state displays, in detectors for the infrared range, or in other possible optoelectronic devices.[9] Trivalent holmium possesses several energy levels in the NIR portion of the spectrum that can be pumped with NIR radiation along with several metastable energy levels ($^5I_6$ and $^5I_7$), which act as good population reservoirs for possible energy-transfer upconversion (ETU) or excited-state absorption (ESA) processes. Consequently, there has been a great deal of interest recently in Ho^{3+}-doped crystals and glasses as upconversion materials.[9,10] Several others have demonstrated continuous wave (cw) green upconversion lasing from Ho^{3+}-doped glass fibers pumped with red light.[11−14]

In previous studies we have investigated in detail the emission and upconversion spectra of Er^{3+}-doped cubic Y_2O_3 and Lu_2O_3 nanocrystals.[15−17] Others have examined the upconversion of Er^{3+} in sol−gel-derived nanocrystalline $BaTiO_3$ powders.[18] To our knowledge, no detailed study of the upconversion properties of Ho^{3+} in a nanocrystal host has yet been performed. In this paper we discuss and report the optical properties of Ho^{3+}-doped cubic Y_2O_3 nanocrystals in an attempt to further broaden the understanding of these novel materials.

2. Experimental Section

2.1. Sample Preparation. Nanosized Y_2O_3 crystals doped with 0.1, 0.5, 1, 2, 5, and 10 mol % Ho_2O_3 ($Y_{1.998}Ho_{0.002}O_3$, $Y_{1.99}Ho_{0.01}O_3$, $Y_{1.98}Ho_{0.02}O_3$, $Y_{1.96}Ho_{0.04}O_3$, $Y_{1.9}Ho_{0.1}O_3$, and $Y_{1.8}Ho_{0.2}O_3$, respectively) were prepared using a solution combustion synthesis procedure.[4,19] Details of the synthesis have been given in a previous article.[15] The synthesis reaction is

$$6M(NO_3)_3 + 10NH_2CH_2COOH + 18O_2 \rightarrow 3M_2O_3 + 5N_2 + 18NO_2 + 20CO_2 + 25H_2O$$

where M = Y, Ho. A glycine-to-metal nitrate molar ratio of 1.2:1 was employed to prepare the aqueous precursor solution. According to the literature, this nitrate-rich composition should allow the formation of small-size yttria particles.[4,19] After the combustion, the powders were fired for 1 h at 500 °C to decompose the residual nitrate ions.

For comparison purposes, bulk $Y_{1.98}Ho_{0.02}O_3$ and $Y_{1.8}Ho_{0.2}O_3$ samples were prepared by conventional solid-state reaction. An appropriate amount of powders of Y_2O_3 (Aldrich, 99.99%) and Ho_2O_3 (Aldrich, 99.99+%) were intimately mixed, pressed into pellets under 10 tons of pressure, and fired in air at 1500 °C for 48 h. At this temperature, the optimum homogeneity (verified using scanning electron microscopy) was obtained. Spectroscopic measurements were carried out also on these samples, which had undergone this heat treatment.

All yttria samples were kept in air without any further precaution.

2.2. IR Spectroscopy. The diffuse reflectance spectrum in the IR region was measured using a Nicolet Magna 760 FTIR spectrometer with a resolution of 2 cm^{-1}. The sample was carefully mixed with KBr (about 5%) and the spectrum was measured using pure KBr as a reference.

2.3. Luminescence Spectroscopy. Luminescence spectra were measured by exciting either at 457.9 nm using a Coherent Sabre Innova, 20 W argon ion laser, at 754 nm using a Spectra-Physics Model 3900 Titanium Sapphire pumped by the 514-nm line of a Coherent Sabre Innova argon ion laser, or at 646 nm using a Spectra-Physics 375 dye laser operating with DCM (Exciton), also pumped by the 514-nm line of the argon laser. The concentration of the dye was 1.2×10^{-3} mol/dm^3 in a mixture of benzyl alcohol/ethylene glycol (3:7) (Aldrich, spectrophotometric, 99+%). The visible emissions were then collected and dispersed using a Jarrel-Ash 1-m Czerny Turner double monochromator. The signals were monitored with a thermoelectrically cooled Hamamatsu R943-02 photomultiplier tube. A preamplifier, model SR440 Stanford Research Systems, processed the photomultiplier signals and a gated photon counter model SR400 Stanford Research Systems data acquisition system was used as an interface between the computer and the spectroscopic hardware.

2.4. Luminescence Decay Times Measurements. Luminescence decay times were measured at each of the excitation wavelengths by modulating the excitation light with a chopper (SR540 Stanford Research Systems). They were recorded using the same gated photon counter mentioned previously.

3. Results and Discussion

3.1. Particle Size. The average crystallite sizes of the end members of the series under investigation, $Y_{1.998}Ho_{0.002}O_3$ and $Y_{1.8}Ho_{0.2}O_3$, were found to be 13 and 10 nm, respectively, from a line-broadening analysis of the 222/444 and 400/800 pairs of X-ray reflections.[20] Moreover, the particle size for $Y_{1.8}Ho_{0.2}O_3$ was confirmed by a detailed structural investigation carried out by small-angle X-ray diffraction and electron microscopy.[20] It is therefore reasonable to assume that the sizes of the other members of the series are comparable to these values as the present synthetic technique appears to be remarkably reproducible and to yield particle sizes which are independent of the chemical identity and concentration of the lanthanide dopant.[19−21] On the other hand, the size of the particles in the bulk sample is at least 10 times larger.

3.2. Luminescence Spectroscopy. The room-temperature visible luminescence spectra of bulk and nanocrystalline samples excited at 457.9 nm are shown in parts a and b, respectively, of Figure 1. The spectra exhibit four distinct emission bands. Blue emission was observed between 480 and 500 nm, corresponding to the $^5F_3 \rightarrow {}^5I_8$ transition. The yellow emission in the region of 530−580 nm is attributed to the transition from the thermalized $^5F_4$ and $^5S_2$ states to the $^5I_8$ ground state.

(9) Kuck, S.; Sokolska, I. *Chem. Phys. Lett.* **2000**, *325*, 257−263.
(10) Malinowski, M.; Wnuk, A.; Frukacz, Z.; Chadeyron, G.; Mahiou, R.; Guy, S.; Joubert, M. F. *J. Alloys Compd.* **2001**, *323−324*, 721−735.
(11) Allain, J. Y.; Monerie, M.; Poignant, H. *Electron. Lett.* **1990**, *26*, 261−262.
(12) Funk, D. S.; Eden, J. G. *IEEE J. Sel. Top. Quantum* **1995**, *1*, 784−791.
(13) Funk, D. S.; Stevens, S. B.; Wu, S. S.; Eden, J. G. *IEEE J. Quantum Electron.* **1996**, *32*, 638−645.
(14) Funk, D. S.; Eden, J. G.; Osinski, J. S.; Lu, B. *Electron. Lett.* **1997**, *33*, 1958−1960.
(15) Capobianco, J. A.; Vetrone, F.; D'Alesio, T.; Tessari, G.; Speghini, A.; Bettinelli, M. *Phys. Chem. Chem. Phys.* **2000**, *2*, 3203−3207.
(16) Capobianco, J. A.; Vetrone, F.; Boyer, J. C.; Speghini, A.; Bettinelli, M. *J. Phys. Chem. B* **2002**, *106*, 1181−1187.
(17) Capobianco, J. A.; Vetrone, F.; Boyer, J. C.; Speghini, A.; Bettinelli, M. *Opt. Mater.* **2002**, *19*, 259−268.
(18) Zhang, H. X.; Kam, C. H.; Zhou, Y.; Han, X. Q.; Buddhudu, S.; Lam, Y. L. *Opt. Mater.* **2000**, *15*, 47−50.
(19) Tessari, G.; Bettinelli, M.; Speghini, A.; Ajò, D.; Pozza, G.; Depero, L. E.; Allieri, B.; Sangaletti, L. *Appl. Surf. Sci.* **1999**, *144−145*, 686−689.
(20) Polizzi, S.; Fagherazzi, G.; Battagliarin, M.; Bettinelli, M.; Speghini, A. *J. Mater. Res.* **2001**, *16*, 146−154.
(21) Fagherazzi, G.; Polizzi, S.; Bettinelli, M.; Speghini, A. *J. Mater. Res.* **2000**, *15*, 586−589.

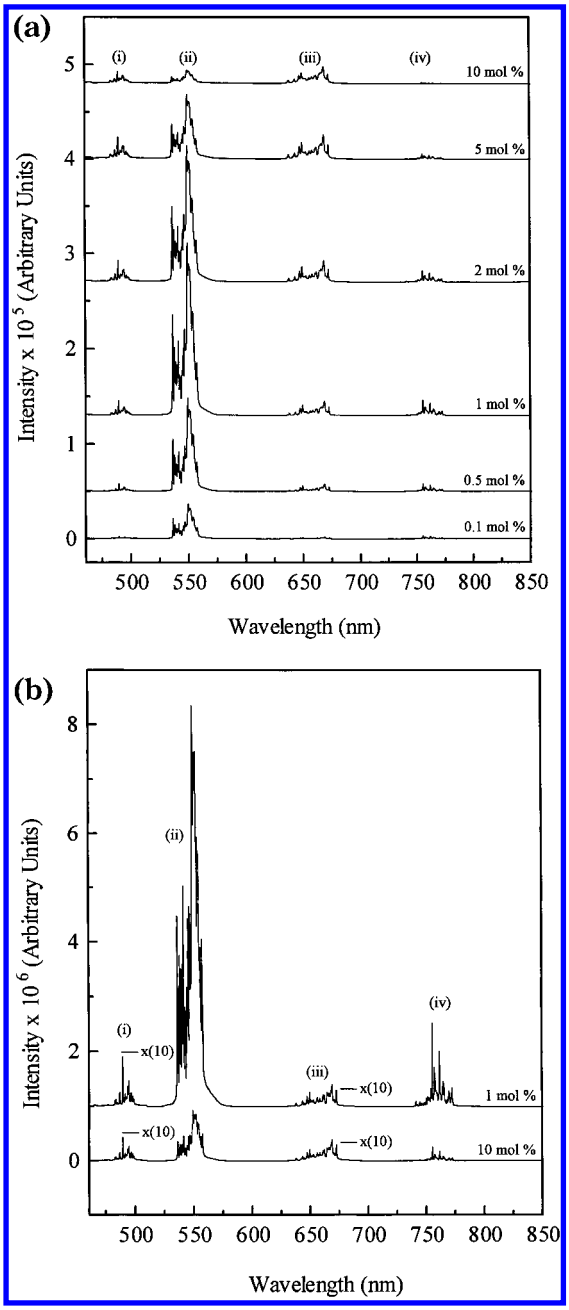

Figure 1. (a) Room-temperature luminescence of bulk Y_2O_3:Ho^{3+} upon excitation at 457.9 nm. (i) $^5F_3 \rightarrow {}^5I_8$; (ii) ($^5F_4$, $^5S_2$) $\rightarrow {}^5I_8$; (iii) $^5F_5 \rightarrow {}^5I_8$; (iv) ($^5F_4$, $^5S_2$) $\rightarrow {}^5I_7$. (b) Room-temperature luminescence of nanocrystalline Y_2O_3:Ho^{3+} upon excitation at 457.9 nm. (i) $^5F_3 \rightarrow {}^5I_8$; (ii) ($^5F_4$, $^5S_2$) $\rightarrow {}^5I_8$; (iii) $^5F_5 \rightarrow {}^5I_8$; (iv) ($^5F_4$, $^5S_2$) $\rightarrow {}^5I_7$.

Red emission was observed between 630 and 680 nm, corresponding to the $^5F_5 \rightarrow {}^5I_8$ transition. NIR emission was observed between 735 and 775 nm, corresponding to the transition from the thermalized $^5F_4$ and $^5S_2$ states to the $^5I_7$ excited state. The transition energies were similar for both the nanocrystalline and bulk samples and there is no noticeable shifting of peaks in any of the samples. The crystal field splitting is therefore reasonably similar for the nanocrystalline and bulk samples.

When the emission spectra of the bulk samples are compared to those of the nanocrystals, one notices that the relative intensities of the peaks do change considerably. In the 1 mol % doped nanocrystalline sample the integrated intensity of the ($^5F_4$, $^5S_2$) $\rightarrow {}^5I_8$ transition was roughly 10 times that of the $^5F_5 \rightarrow {}^5I_8$ transition, while in the 1 mol % doped bulk sample the ratio of the relative intensities of these two transitions was ≈150:1. One also notices that the overall luminescence is severely reduced by about 1 order of magnitude in the nanocrystal samples compared to that of the bulk samples. In a previous paper on Y_2O_3:Er^{3+} nanocrystals we have attributed this type of behavior to an increase in multiphonon relaxation due to adsorbed atmospheric carbon dioxide and/or water.[15]

Similar to the Y_2O_3:Er^{3+} nanocrystals, the medium IR spectra of the nanocrystalline Y_2O_3:Ho^{3+} samples under investigation show that the materials have adsorbed atmospheric CO_2 and H_2O. In fact, the MIR spectra show bands around 1500 and 3350 cm^{-1}, which can be attributed to stretching modes of carbonate and hydroxide ions. The presence of these ions on the surface of the nanocrystalline materials yields vibrational quanta of higher wavenumbers compared to the intrinsic phonons of yttria (≈600 cm^{-1}), resulting in an increase of multiphonon relaxations from all excited levels under consideration. Because the radiative decay rates for the Ho^{3+} ions in the bulk and nanocrystalline samples should be of the same order of magnitude, the larger nonradiative decay probability in the nanocrystals leads to lower emission efficiencies when compared to their bulk counterparts.

The rapid quenching of the ($^5F_4$, $^5S_2$) $\rightarrow {}^5I_8$ transition relative to the $^5F_5 \rightarrow {}^5I_8$ transition in the nanocrystalline samples can also be attributed to the presence of the adsorbed atmospheric molecules. The conditions necessary for efficient nonradiative decay are well-known.[22] In particular, the energy difference ΔE between the levels in question should be equal to or less than 4−5 times the highest vibrational frequency of the surroundings. The energy gap between the $^5S_2$ and $^5F_5$ levels for the Ho^{3+} ion in Y_2O_3 single crystals[23] has been reported to be 2666 cm^{-1}. As this gap is slightly higher than four high-energy phonons of the bulk material (about 600 cm^{-1}), the $^5S_2$ level is slightly affected by multiphonon decay. In the nanocrystals this gap could be spanned with two of the high-energy carbonate ion phonons available or just one hydroxide high-energy phonon, making multiphonon relaxation of ($^5F_4$, $^5S_2$) levels much more probable than for its bulk counterpart.

The energy gap between the $^5F_5$ and $^5I_4$ levels is just 1793 cm^{-1}. This gap can be spanned by three of the intrinsic yttria phonons, meaning it would undergo a significant amount of nonradiative relaxation already in the bulk sample. The multiphonon relaxation quantum efficiency for this level is ≈1.0 in a Y_2O_3 single crystal.[24] In the nanocrystals the number of phonons needed is reduced to slightly more than one if one considers the high-energy carbonate ion phonons available or just one hydroxide ion high-energy phonon.

In the bulk materials there is a difference of at least one phonon needed for multiphonon decay of the $^5S_2$ and $^5F_5$ levels. If one examines the energy-gap dependence of the spontaneous multiphonon transition rate in

(22) Blasse, G. *Prog. Solid State Chem.* **1988**, *18*, 79−171.
(23) Leavitt, R. P.; Gruber, J. B.; Chang, N. C.; Morrison, C. A. *J. Chem. Phys.* **1982**, *76*, 4775−4788.
(24) Riseberg, L. A.; Moos, H. W. *Phys. Rev.* **1968**, *174*, 429−438.

single-crystal Y_2O_3,[24,25] this would then lead to an $\approx 10^2$ greater multiphonon relaxation rate for the $^5F_5$ level as compared to that of the $^5S_2$ level. In the nanocrystalline samples the same number of phonons is needed either in considering carbonate or hydroxide ion high-energy phonons for the relaxation of both levels. This should result in a similar rate of multiphonon relaxation for the $^5S_2$ and $^5F_5$ levels in the nanocrystalline samples and therefore a quenching of the ($^5F_4$, $^5S_2$) $\rightarrow$ $^5I_8$ transition relative to the $^5F_5 \rightarrow {}^5I_8$ transition when compared to those of the bulk materials.

In a previous study on Er^{3+}-doped nanocrystalline Y_2O_3 different heat treatments were carried out on a nanocrystalline $Y_{1.8}Er_{0.2}O_3$ sample to reduce the amount of carbonate and hydroxide ions on the surface of the nanoparticles.[16] First, the sample was treated at 800 °C for 17 h and subsequently cooled to room temperature. The same sample was then treated at 1000 °C for 65 h and again cooled to room temperature. The MIR spectra of the doped nanocrystalline yttria sample after both heat treatments still showed bands at approximately 1500 and 3350 cm^{-1}, which indicated the presence of carbonate and hydroxide ions, respectively. On the other hand, the bulk sample showed no bands at 1500 and 3350 cm^{-1}, indicating the lack of carbonate and hydroxide ions. A reduction of the overall intensities of the bands at 1500 and 3350 cm^{-1} after both heat treatments was noted, indicating a reduction, not a complete removal, of the overall surface contamination. A consequence of these long heat treatments at higher temperatures is a possible aggregation (combination) of the nanoparticles to form larger particles. This creates a difficulty in comparing the luminescence of heat-treated and non-heat-treated nanocrystalline materials as the spectroscopy of the nanocrystalline material is particle-size-dependent.

When examining the behavior of the relative intensities of the ($^5F_4$, $^5S_2$) $\rightarrow$ $^5I_8$ transition to the $^5F_3 \rightarrow {}^5I_8$ and $^5F_5 \rightarrow {}^5I_8$ transitions in the bulk and nanocrystalline samples, one notices a rapid quenching of the ($^5F_4$, $^5S_2$) $\rightarrow$ $^5I_8$ transition as the Ho^{3+} dopant concentration increases from 1 to 10 mol %. This type of behavior suggests a rapid energy transfer from the ($^5F_4$,$^5S_2$) level. For samples with Ho^{3+} concentration <1 mol %, nonradiative relaxation by ion−ion interactions can be assumed to be negligible. As the concentration increases, the continuous spectral changes observed indicate that interactions between ions develop at doping levels above 1 mol %. By examining the energy levels of Y_2O_3:Ho^{3+},[23] one is capable of elucidating ion-pair cross-relaxation processes that are likely to occur. One such resonant cross-relaxation is represented by the $^5S_2 \rightarrow {}^5I_4$ and $^5I_7 \leftarrow {}^5I_8$ transitions. In this energy transfer process a donor Ho^{3+} ion in the $^5S_2$ excited state relaxes nonradiatively to the $^5I_4$ state, while in another simultaneous nonradiative process an acceptor Ho^{3+} ion in a ground $^5I_8$ state is excited to the $^5I_7$ state, thereby quenching the luminescence of the ($^5F_4$, $^5S_2$) level. This energy transfer from the ($^5F_4$,$^5S_2$) level is well-documented and has also been observed in Ho^{3+}-doped $ZnCl_2$-based glasses[26] and $YAlO_3$:Ho^{3+} crystals.[27] The concentration quenching observed in the nanocrystal samples can be attributed to this cross-relaxation process.

Table 1. Decay Times Obtained from an Exponential Fit of the Room-Temperature Decay Curves for the ($^5F_4$,$^5S_2$) → $^5I_8$ Transition upon 457.9-nm Excitation

sample	decay time (μs)	
bulk		
$Y_{1.98}Ho_{0.02}O_3$	135	
$Y_{1.80}Ho_{0.20}O_3$	60	
nanocrystalline	first decay time (μs)	second decay time (μs)
$Y_{1.998}Ho_{0.002}O_3$	17	77
$Y_{1.99}Ho_{0.01}O_3$	20	73
$Y_{1.98}Ho_{0.02}O_3$	14	57
$Y_{1.96}Ho_{0.04}O_3$	9	40
$Y_{1.90}Ho_{0.10}O_3$	3	14
$Y_{1.80}Ho_{0.20}O_3$	2	4

3.3. Emission Decay Times. Room-temperature emission decay curves of the ($^5F_4$, $^5S_2$) $\rightarrow$ $^5I_8$ transition upon 457.9-nm excitation were monitored for both the bulk and nanocrystalline samples. The lifetimes are reported in Table 1. Decay curves for the bulk samples were fitted with a single-exponential model. However, a deviation from first-exponential behavior was observed in all decay curves obtained for the nanocrystalline samples. The difficulty in fitting with a single-exponential model in the more diluted nanocrystalline samples (0.1−2 mol %) arises because there is a distribution of dopant ions within the individual nanocrystals that are coupled in various degrees to the absorbed surface molecules. The dopant ions located close to the surface would have a faster decay than those ions located inside the nanocrystals. This distribution of ions thus leads to a nonexponential decay as a significant portion of the dopant atoms reside near the surface because of the particles' small size (about 10 nm).

It is possible to fit the curves of the nanocrystalline samples with a double-exponential model because, theoretically, one would expect two time constants: one for the ions at the surface and a second for the ions inside the nanocrystals. The value of the first time constant is relatively low with respect to the second one and both remain reasonably constant in the low-concentration regime (0.1−1 mol %). This behavior is not observed in the samples with dopant concentrations >1 mol % as the decay process is now influenced by the energy-transfer process between the holmium ions.

Both time constants decrease steadily as the concentration of the dopant ion is raised. As the concentration of the dopant ion is increased up to 5 mol %, the deviation from first-order exponential behavior increases as interactions between the dopant ions become significant. As mentioned previously, a strong cross-relaxation process involving energy transfer between two holmium ions is observed, which depopulates the ($^5F_4$, $^5S_2$) level. This process increases the rate of nonradiative relaxations, thus explaining the rapid decrease of the lifetime of this level with increasing Ho^{3+} concentration.

The lifetimes of the excited states were found to be significantly faster in the nanocrystal samples than in the bulk samples. For example, the ($^5F_4$, $^5S_2$) $\rightarrow$ $^5I_8$ lifetime in the 1 mol % bulk sample was found to be

(25) Weber, M. J. *Phys. Rev.* **1968**, *171*, 283−291.
(26) Shojiya, M.; Kawamoto, Y.; Kadona, K. *J. Appl. Phys.* **2001**, *89*, 4944−4950.
(27) Malinowski, M.; Piramidowicz, R.; Frukacz, Z.; Chadeyron, G.; Mahiou, R.; Joubert, M. F. *Opt. Mater.* **1999**, *12*, 409−423.

135 μs as opposed to 14 μs (first time constant) or 57 μs (second time constant) in the similarly doped nanocrystalline sample. The lifetime of an excited state a is given by

$$\frac{1}{\tau_c} = \sum_b (A_{ab} + W_{ab})$$

where A_{ab} and W_{ab} are the radiative and nonradiative transition probabilities, respectively, from level a to level b, and the summation is over all terminal levels b.[28] Nonradiative processes include multiphonon relaxations and energy transfer between ions. Differences in the rate of nonradiative decay from a given rare-earth level arise from the highest phonon energy available in the sample and the number of phonons required to bridge the energy gap. Because phonons of higher energy are present in the nanocrystals as opposed to the bulk samples, nonradiative transitions from the ($^5F_4$, $^5S_2$) level to the $^5F_5$ level will require a lower order multiphonon process, resulting in a rapid relaxation. This accounts for the larger rate of nonradiative processes in the nanocrystalline samples for a given size energy gap. The resulting lifetime of the ($^5F_4$, $^5S_2$) level is therefore shorter.

3.4. Upconversion upon Excitation into the $^5F_5$ Manifold. Upon excitation with 646-nm radiation from a dye laser that populates the $^5F_5$ level, anti-Stokes emission corresponding to the $^5F_3 \rightarrow {}^5I_8$ and ($^5F_4$, $^5S_2$) $\rightarrow {}^5I_8$ transitions were observed. The luminescence spectra of the bulk and nanocrystalline samples are shown in parts a and b of Figure 2, respectively. The intensity of the upconverted luminescence I_0 is proportional to some power n of the pump intensity I_i($I_0 \propto I_i^n$)[29] where n, which is called the order of the upconversion process, is the number of pump photons required to populate the emitting state. The intensity of the upconverted blue and green emission has been measured as a function of the 646-nm excitation intensity. From a fit of the curve ln I_i versus ln I_0 we have obtained a slope of 1.9, which indicates a two-photon upconversion process, as shown in Figure 3.

The decay times of the ($^5F_4$, $^5S_2$) $\rightarrow {}^5I_8$ upconversion transition are identical to those obtained with 457.9-nm excitation for all the concentrations. No change in the relative intensity of the blue and green luminescence between the direct emission and upconversion spectra is observed. An energy-transfer upconversion (ETU) process seems to be unlikely because the upconversion luminescence decreases with increasing Ho^{3+} concentration. If an ETU process were occurring, the luminescence should increase with increasing dopant concentration as the distance between the holmium atoms would decrease, thus favoring energy transfer. A photon avalanche upconversion process is also ruled out as no power threshold for the upconversion luminescence is observed. On the basis of these observations, we propose that the upconversion most probably results from an excited-state absorption (ESA) process.

The $^5I_5$, $^5I_6$, and $^5I_7$ multiplets are typically long-lived with appropriate energy gaps to upper emitting levels.

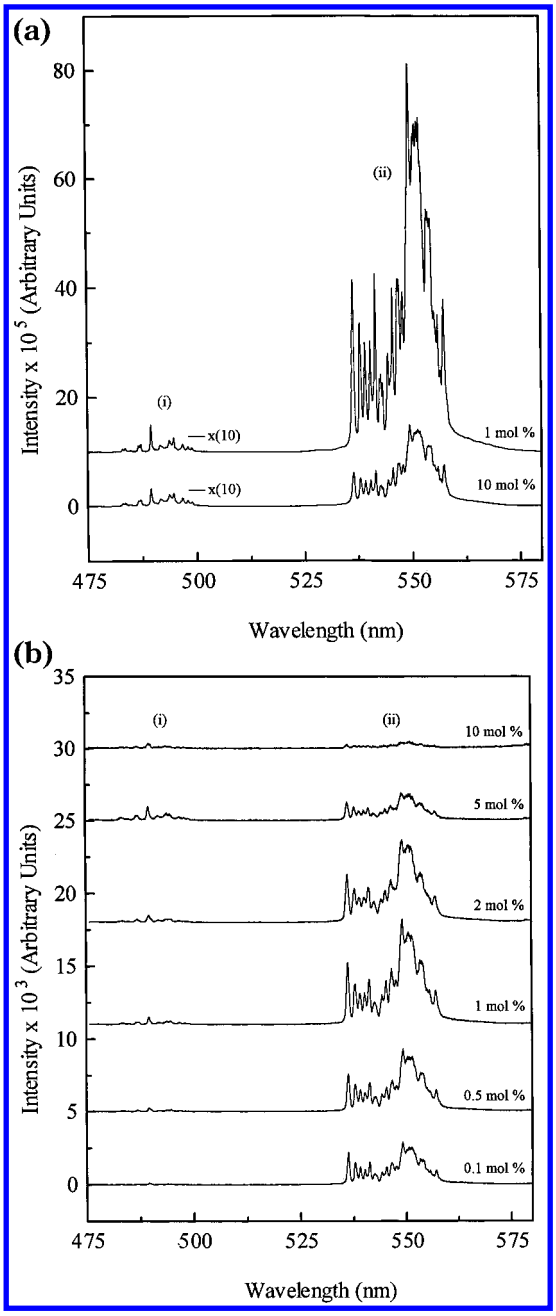

Figure 2. (a) Upconverted emission of bulk Ho^{3+}-doped Y_2O_3 at room temperature upon 646-nm excitation, showing (i) $^5F_3 \rightarrow {}^5I_8$ and (ii) ($^5F_4$, $^5S_2$) $\rightarrow {}^5I_8$. (b) Upconverted emission of Ho^{3+}-doped Y_2O_3 nanocrystals at room temperature upon 646-nm excitation, showing (i) $^5F_3 \rightarrow {}^5I_8$ and (ii) ($^5F_4$, $^5S_2$) $\rightarrow {}^5I_8$.

For 646-nm excitation excited-state absorption from $^5I_7$ is most likely to occur because there is appropriate resonance $^5I_7 \rightarrow {}^5F_3$. The mechanism by which the ($^5F_4$, $^5S_2$) and $^5F_5$ levels are populated is assigned as follows (see Figure 5). The laser light brings the Ho^{3+} ion into the $^5F_5$ level, which then nonradiatively decays to the $^5I_7$ level. An excited-state absorption process brings the ion to the $^5F_3$ level. The ion then emits through the $^5F_3 \rightarrow {}^5I_8$ transition or can nonradiatively decay to the lower lying levels and the ($^5F_4$, $^5S_2$) $\rightarrow {}^5I_8$ transition occurs.

The upconversion process was noted to be far less efficient in the nanocrystal samples. This decrease in luminescence is attributed to an increase of multiphonon relaxations of excited levels because of the

(28) Layne, C. B.; Lowdermilk, W. H.; Weber, M. J. *Phys. Rev. B* **1977**, *16*, 10−20.
(29) Chamarro, A.; Cases, R. *J. Lumin.* **1990**, *46*, 59.

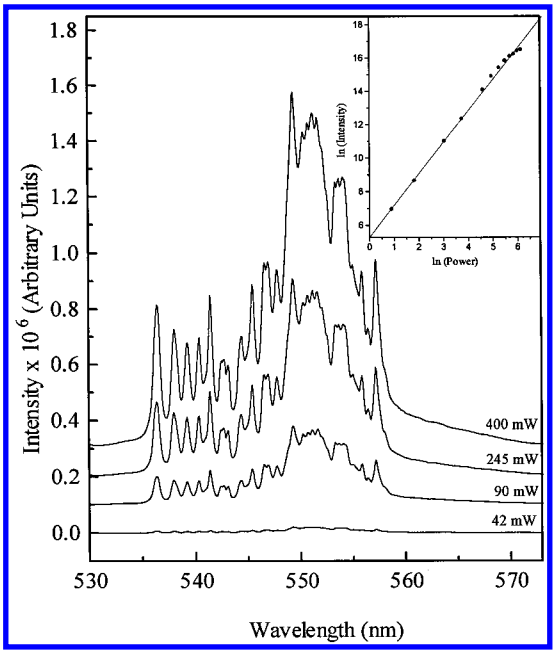

Figure 3. Power study of the ($^5F_4$, $^5S_2$) → $^5I_8$ transition in 10 mol % bulk Y_2O_3:Ho^{3+} at room temperature upon 646-nm excitation. Inset: Power dependence of the upconversion luminescence intensity observed with 646-nm excitation.

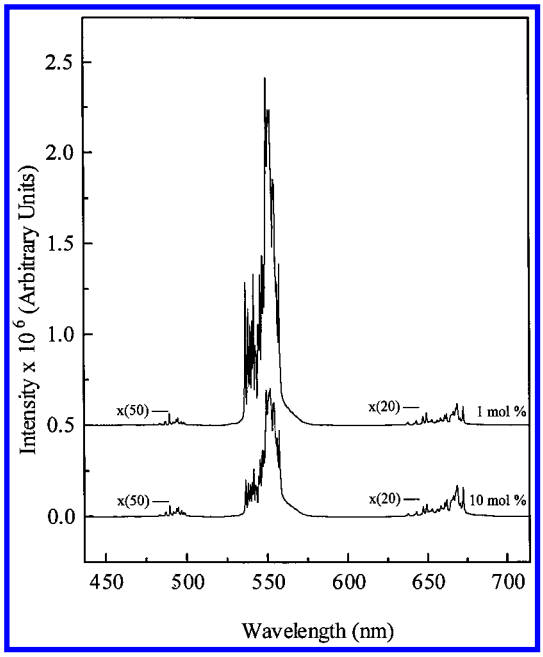

Figure 4. Upconverted emission of bulk Ho^{3+}-doped Y_2O_3 at room temperature upon 754-nm excitation, showing (i) $^5F_3$ → $^5I_8$, (ii) ($^5F_4$, $^5S_2$) → $^5I_8$, and (iii) $^5F_5$ → $^5I_8$.

presence of carbonate and hydroxide ions on the surface of the nanocrystals. The populations of the intermediate levels from which a part of the excited ions can be re-excited to the upper emitting levels by excited-state absorption (ESA) are substantially impacted by the nonradiative decay rate that increases as the lattice phonon energy becomes higher.[30] The highest available phonon energy not only affects quantum efficiencies of the emitting levels such as $^5F_3$ and $^5S_2$ levels but also impacts the upconversion efficiencies, which are primarily determined by populations of intermediate levels such as the $^5I_6$ and $^5I_7$. The excitation populations of intermediate levels and the quantum efficiencies of emitting levels of Ho^{3+} in a host crystal with a higher phonon energy are undoubtedly lower than those in a crystal with a lower phonon energy.

3.5. Upconversion upon Excitation into the $^5I_4$ Manifold. Upon excitation with 754-nm radiation from a titanium sapphire laser that excites the $^5I_4$ level, anti-Stokes emission corresponding to the $^5F_3$ → $^5I_8$, ($^5F_4$, $^5S_2$) → $^5I_8$, and $^5F_5$ → $^5I_8$ transitions were observed in the bulk samples. The luminescence spectra are shown in Figure 4. Though strong luminescence was observed from the bulk samples, no upconversion was noted in the nanocrystal samples. As mentioned previously, behavior of this type is attributed to an increase of multiphonon relaxations of excited levels because of the presence of carbonate and hydroxide ions on the surface of the nanoparticles.

The ($^5F_4$, $^5S_2$) → $^5I_8$ transition demonstrated a quadratic dependence on the power of the pump beam, indicating that two photons were involved in the excitation process. Again, an excited-state absorption (ESA) process is thought to be the dominant mechanism for the same reasons mentioned previously for upconversion

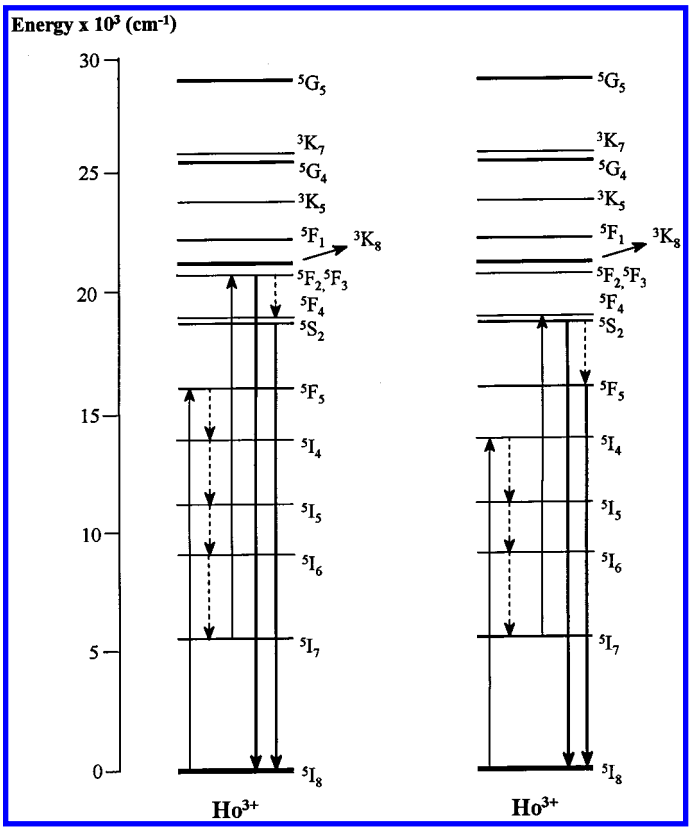

Figure 5. Two excitation mechanisms for Ho^{3+} upconversion in Y_2O_3: (left) 646-nm excitation, resulting in excited state absorption via the $^5I_7$ level; (right) 754-nm excitation resulting in excited state absorption via the $^5I_7$ level.

using 646-nm radiation: the decay times of the ($^5F_4$, $^5S_2$) → $^5I_8$ upconversion transition are identical to those obtained with 457.9-nm excitation; no power threshold for the upconversion emission was noted and the upconversion luminescence decreases with increasing Ho^{3+} concentration.

(30) Hirao, K.; Kishimoto, S.; Tanaka, K.; Tanabe, S.; Soga, N. *J. Non-Cryst. Solids* **1992**, *139*, 151−156.

Another possible reason mentioned previously for justifying an ESA process, no change in the relative intensity of the blue and green luminescence between the direct emission and upconversion spectra, does not apply in this case but can easily be explained. The relative intensity of the blue emission transition compared to the green one is severely reduced upon 754-nm excitation. The reason for this behavior is that there are two distinct ESA processes occurring concurrently that originate from the $^5I_6$ and $^5I_7$ levels and could populate the $^5G_6$, $^3K_8$, and ($^5F_4$, $^5S_2$) levels, respectively. It is well-known that the $^5I_7$ level possesses a longer lifetime and a larger radiative character than the $^5I_6$ level; thus, excited-state absorption from $^5I_7$ rather than the $^5I_6$ level is most likely to occur. Therefore, the proposed mechanism is the following (Figure 5). The laser light brings the Ho^{3+} ion into the $^5I_4$ level, which then nonradiatively decays to the $^5I_7$ level. An excited-state absorption process brings the ion to the ($^5F_4$, $^5S_2$) levels. The ion then emits through the ($^5F_4$, $^5S_2$) $\rightarrow$ $^5I_8$ transition or can nonradiatively decay to the lower lying levels and the $^5F_5 \rightarrow {}^5I_8$ transition occurs. This mechanism is further aided by an increase in the population of the $^5I_7$ level via the cross-relaxation mechanism mentioned previously. The increase in the population of the $^5I_7$ level leads to the efficient population of the ($^5F_4$, $^5S_2$) levels through the ESA process and to the intense green emission. A second ESA process originating from the $^5I_6$ level is also possible. For the 754-nm excitation wavelength used in this study there is another possible resonant excited-state absorption: $^5I_6 \rightarrow {}^3K_8$, $^5G_6$. It is most likely that this ESA process along with nonradiative relaxation is responsible for the weak blue emission from the $^5F_3$ level noted in Figure 3.

Conlusions

Emission spectra and lifetimes of the excited states of the nanocrystal samples differ significantly from those of the bulk. The upconverted intensity at both excitation wavelengths was found to decrease with increasing holmium concentration, which suggests a ESA-type mechanism. Upconversion processes are far less efficient, or nonexistent, in the nanocrystalline samples because of the presence of carbonate ions and water on the surface. The bulk material shows enhanced green emission ($^5F_4$, $^5S_2 \rightarrow {}^5I_8$) over its nanocrystal counterpart in both the emission and upconversion spectra.

Acknowledgment. The authors gratefully acknowledge the Natural Science and Engineering Research Council of Canada and MURST (Project 9903222581_005) of Italy, for financial support. The authors gratefully thank Erica Viviani (Università di Verona) for expert technical assistance and Stefano Polizzi (Università di Venezia) for the X-ray analysis of the samples.

CM011584M